Atomistic simulation of defects in alkaline-earth fluorohalide crystals

Roger C. Baetzold
Corporate Research Laboratories, Eastman Kodak Company, Rochester, New York 14650
(Received 24 June 1987)

Defect properties of BaFBr, BaFCl, and SrFCl were calculated using the atomistic simulation technique. Two-body potentials were developed starting from potentials in related crystals or calculated by the electron-gas method and then fit to minimize strain in the equilibrium structure. Agreement of calculated elastic, dielectric, and cohesive properties with available experimental and theoretical data was reasonable. Generally, Frenkel energies for the larger-size halogen ion were less than for the fluorine ion and less than the Schottky energy for the metal, fluoride, and other halide ions set. A Schottky energy for vacancies of the metal ion and two of the larger-size halide ions was small. Energies of formation of V_k and H centers were computed with the aid of thermodynamic cycles. The most stable V_k center forms on the halide ion site where the Madelung potential is most favorable for holes. H centers occupy off-center sites in these low-symmetry materials. Stable geometries are discussed.

I. INTRODUCTION

The alkaline-earth fluorohalides are an important class of materials having the matlochkite structure.[1] A wide range of compositions involving cations including Ca^{2+}, Sr^{2+}, Eu^{2+}, and Ba^{2+} with the anions F^-, Cl^-, Br^-, and I^- have been prepared.[2] These compounds have long been of interest because of the various charged defect species which can be detected by spin resonance and associated techniques.[3–6] A theoretical analysis of these centers has appeared.[7] Other physical properties, including long-wavelength dynamics,[8] dielectric dispersion,[9] and elastic constants,[10] have been reported for some members of the series. While several physical properties are available, there is far from a complete characterization of this class of materials.

The luminescent properties of the mixed halide–alkaline-earth compounds have recently been discussed as the basis for phosphor materials.[11–13] This effect is based upon the property of photostimulated luminescence possessed by these materials. Thus in addition to the considerable scientific interest in these materials, there is also potential technological application.

The mechanism of excitation and luminescent decay in the alkaline-earth fluorohalides depends upon the energetics of various charged and neutral defect species. Many of these defects have been discussed in relation to properties measured in alkali halides.[14–16] An exciton is formed from excitation of electrons by a photon of appropriate energy and consists of the electron bound to a hole center. One mechanism of exciton decay leads to F and H centers which are able to move apart at sufficiently high temperature. The F center is an electron trapped at a halide ion vacancy and the H center is a hole in the form of a halogen molecular anion trapped on a lattice site. The self-trapped hole or V_k center consists of a hole shared between two adjacent halide ions that have moved towards one another. In addition to these electronic defects there are also ionic defects consisting of ion vacancies or interstitial ions.

The purpose of this report is to examine energetics of various ionic and electronic defects in alkaline-earth fluorohalide materials using an atomistic simulation method. Hole defects can be treated by this method because of their strong localization. Defects involving electrons will be treated in a future report by applying a Hartree-Fock lattice method.[17] The electron defect, such as an F center, has considerable electronic delocalization on host lattice ions and cannot be treated by atomistic techniques which normally do not provide for diffuse electron distributions.

II. METHOD

The method of atomistic simulation has been fully documented in the literature,[18,19] and we have described applications to specific problems.[20] Thus only a brief review will be considered here. A defect in an ionic solid possesses a long-range interaction with the host lattice ions. This feature is included in these calculations through the Mott-Littleton approach. This approach divides space around a defect into a spherical region immediately enclosing the defect within which full spatial relaxation of all ions is allowed. This region typically consists of 100–200 ions and is referred to as region I. Surrounding this sphere is a second sphere extending 5–7 lattice constants in radius. Within this region IIA a harmonic relaxation technique is employed. Finally, the rest of the crystal is treated with continuum approaches. This total procedure is encompassed within the HADES (Ref. 19) computer code.

Polarization of all lattice ions is treated in this calculation by the shell model.[21] Thus each ion consists of a core and massless shell of charge which are connected by a harmonic spring constant. The shell can displace from the core causing a dipole and leading to a proper description of the crystal dielectric behavior.

The Coulomb and short-range interactions between

 ©1987 The American Physical Society

ions in alkaline-earth halides have been successfully treated by two-body potentials.[18,22] These potentials will be a starting point for the potentials which will be developed for the alkaline-earth fluorohalides. Thus an assumption of transferability of potentials from different crystals will be invoked. We also note that only central-force potentials will be employed, because in general they have proven adequate for the alkaline-earth halides.[23]

Let us consider the general question of constructing potentials for short-range ion interaction in crystals. The electron gas[24] method of calculation has been widely used to determine potentials theoretically. *Ab initio* methods of calculation have been employed in a limited number of cases. The most widespread method has involved empirical potentials which are determined by fitting to perfect crystal physical properties. We will discuss the specific applications of these methods to alkaline-earth fluorohalides later.

III. RESULTS

A. Potentials

Several mixed alkaline-earth halides possess a tetragonal structure of which PbFCl is the prototype. This structure, often termed matlochkite, is shown in Fig. 1 for barium fluorobromide. Good structural information obtained by x-ray diffraction has been reported[1] for several compounds of this type, including BaFBr, SrFCl, and BaFCl. It can be pointed out from the unit cell in Fig. 1 that the C axis is perpendicular to planes of like ions. Alternating Ba^{2+} and F^- planes exist, but two adjacent Br^- planes are present. A cleavage plane forms between the two Br^- planes, but this structure also has

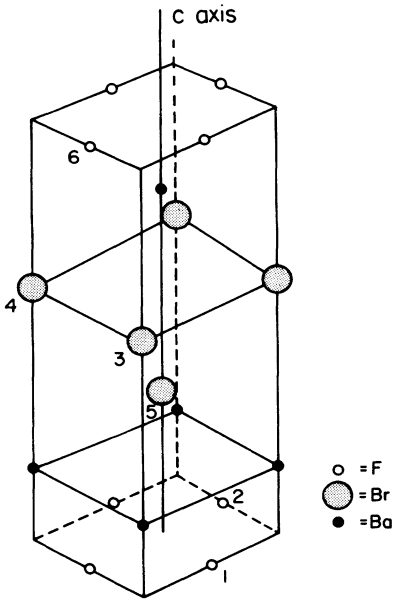

FIG. 1. A sketch of the matlochkite structure for BaFBr is shown. Note that planes of like ions run normal to the crystal C axis.

important consequences for the Madelung potential and therefore carrier trapping properties, as we have pointed out previously.[20] The same structural properties are found in SrFCl and BaFCl where two adjacent Cl^- planes exist.

Two-body potentials used to describe the interactions of ions in a solid have the form

$$\phi_{ij}(r)=\frac{Z_iZ_je^2}{r^2}+Ae^{-r/\rho}-C/r^6\ , \tag{1}$$

where Z_i is the ionic charge, r is the separation of ions i and j and A, ρ, and C are constants of the potential. While the Coulomb term is dominant in the energy, it is the short-range terms that determine the crystal structure.

Consider the basis for developing a potential for BaFBr. Structural data are known, but most of the dielectric, elastic, and piezoelectric data are missing. Thus empirical potentials cannot be devised at this time. The only alternative available involves use of electron-gas potentials and assumptions of transferability from pure alkaline-earth halides. This assumes that a potential used in one crystal structure is unchanged upon usage in a different crystal structure. Stoneham and Harding[22] wrote that while the procedure is often justified, in practice there is no real theoretical basis for this assumption. Also there is the caution about mixing potentials developed by electron-gas and empirical means. Despite these cautions, we begin with this starting point.

We consider the starting point for obtaining a potential for BaFBr as a representative example for all of the materials considered in this report. Table I shows a schematic of the starting point for the BaFBr potential. Several parameters are taken from BaO, BaF_2, and KBr known potentials whenever these are available.[25] The electron-gas method is used to obtain repulsive interactions for Ba-Br and F-Br. Then the attractive terms [C in Eq. (1)] are varied to obtain the lowest possible strain at the experimental BaFBr structure. This procedure does not guarantee a global minimum in parameter space but does guarantee a fit to crystal properties. Parameters for the shell model are taken from the known potentials and primarily determine the dielectric constants. Experimental dielectric and elastic constants would be needed to assess this potential in more detail. Comparison of this potential (I) to typical alkali-halide potentials[25] reveals many similarities but somewhat

TABLE I. Source of BaFBr potential. Source of potential in parentheses.

Interaction	A	ρ	C
Ba-Ba	(Ba-O)	(Ba-O)	Fit[b]
Ba-F	(BaF_2)	(BaF_2)	Fit[b]
F-F	(BaF_2)	(BaF_2)	Fit[b]
Ba-Br	(EG)[a]	(EG)[a]	Fit[b]
F-Br	(EG)[a]	(EG)[a]	Fit[b]
Br-Br	(KBr)	(KBr)	(KBr)

[a]Electron-gas calculation.
[b]Fit to minimize lattice strain.

TABLE II. BaFBr potentials.

Potential	Interaction	A (eV)	ρ (Å)	C (eV Å^6)
I	Ba-Ba	588 445.0	0.2070	42.8
II		590 482.2	0.2054	10.7
I	Ba-F	5193.3	0.2795	31.5
II		5193.3	0.2795	0.0
I	F-F	1227.7	0.2753	20.9
II		1228.3	0.2757	149.7
I	Ba-Br	4431.0	0.3644	477.5
II		4350.2	0.3628	236.5
I	F-Br	3588.0	0.3815	829.4
II		2003.0	0.2813	26.0
I	Br-Br	2745.0	0.3986	387.3
II		2948.7	0.3165	194.3

Shell constants

	Shell charge	Force constant (eV/Å^2)
Ba^{2+}	−16.99	1709.1
F^-	−2.38	101.2
Br^-	−2.094	18.30

larger van der Waals terms. In an attempt to provide a range of results we developed a second potential (II) by suppressing the C values and refitting. This leads to potential II in Table II. Use of both potentials to compute BaFBr properties will provide a range of values showing the sensitivity of a property to a potential.

Now let us consider BaFCl and SrFCl which, as we noted earlier, have the same crystal structure as BaFBr. We begin with the same general procedure employing transferability and electron gas as the starting point of our potential and then fitting to minimize lattice strain. The final potentials are shown in Table III. We may compare properties computed by this procedure with perfect crystal properties in Table IV. In the case of elastic constants[10] there is quite good agreement with prior calculated values for BaFCl and SrFCl. Some discrepancies are apparent, but the general trends are reproduced well. The dielectric constant data obtained directly or by calculation from Ref. 9 also agree well with BaFCl computed data. This procedure seems to give satisfactory potentials although we do not claim it to be unique. Attempts to improve the fit to BaFCl or SrFCl elastic data by a least-squares method did not yield a significant improvement. Thus we have retained

TABLE III. Potentials for BaFCl and SrFCl.

	A (eV)	ρ (Å)	C (eV Å^6)
		BaFCl potential	
Ba-Ba	588 445.0	0.2070	0.0
Ba-F	5193.3	0.2795	0.0
F-F	1127.7	0.2753	155.0
Ba-Cl	4431.1	0.3644	532.0
F-Cl	1200.0	0.3000	46.3
Cl-Cl	1227.2	0.3214	172.0
		SrFCl potential	
Sr-Sr	27 334.8	0.2897	76.5
Sr-F	2303.6	0.2919	0.0
F-F	507.5	0.1416	90.7
Sr-Cl	2274.2	0.3423	49.8
F-Cl	1218.0	0.3073	49.8
Cl-Cl	1217.6	0.3198	70.8

	Shell charge	Force constant (eV/Å^2)
Sr^{2+}	−5.53	646.52
Ba^{2+}	−16.99	1709.1
F^-	−2.38	101.2
Cl^-	−2.519	29.38

TABLE IV. Computed properties of various mixed halide crystals. Values in parentheses represent previous data.

Property	BaFBr Potential I	BaFBr Potential II	BaFCl	SrFCl
Elastic coefficients[a] (10^{11} dyn/cm^2)				
C_{11}	8.64	7.88	8.75 (9.08)	11.08 (0.61)
C_{12}	2.84	2.01	2.43 (2.67)	1.54 (3.32)
C_{13}	4.64	3.49	4.69 (4.16)	4.76 (4.58)
C_{33}	7.06	7.09	8.50 (6.00)	9.56 (8.29)
C_{44}	3.07	1.97	1.21 (2.43)	2.99 (3.06)
C_{66}	2.69	2.53	3.09 (3.32)	2.14 (3.79)
ϵ_0[b]	8.61,7.61	5.29,5.29	6.96,6.67(5.9)	6.23,6.15
ϵ_∞[b]	2.61,2.51	1.69,1.64	2.81,2.73(2.7)[f]	1.59,1.58
E_{coh} (eV)[c]	23.8	22.6	23.8	23.9
a_0 (Å)[d]	4.508 (4.508)	4.513	4.38 (4.38)	4.088 (4.088)
BLS[e]	0.006	0.001	0.001	0.008

[a]Reference 10.
[b]Dielectric constants (Ref. 9).
[c]Cohesive energy (Refs. 26 and 27).
[d]Lattice constant.
[e]Bulk lattice strain.
[f]Estimated from refractive index (Ref. 9).

the original potentials in Tables II and III for all work.

The lattice energies of matlochkite structures, including BaFBr, SrFCl, and BaFCl, have been computed[26,27] using various ionic models. The values are 21.5, 23.9, and 22.6 eV, respectively. There is good agreement with the entries in Table IV, providing additional support for the procedures considered here.

One final point to be discussed concerns the nonzero bulk lattice strain shown in Table IV for all of the potentials. The presence of this strain leads to a nonzero strain energy for the perfect crystal. All defect energies are reported relative to this strain energy. In addition to this procedure, an alternate method allowing separation of core and shell components was applied in order to relax the strain energy to zero. This procedure can then also provide a starting point for the calculations and is discussed in the Appendix.

B. Defects in fluorohalides

We begin studies of defects by considering substitution of halide ions in the lattice. The energy of substitution corresponds to exchanging an ion at infinity with a lattice ion. We observe from Table V that replacing a larger lattice halogen ion by a smaller halogen ion is exothermic and the reverse process is endothermic. The same relations are found for F^- and Cl^- on the BaFCl and SrFCl crystals and seem consistent with ideas based upon ion size. A large ion forces a lattice distortion while a small ion allows the lattice to relax to a lower energy. We have also considered energies of substitution in the binary alkaline-earth halides BaF_2, $BaCl_2$, SrF_2, and $SrCl_2$ where the potential parameters are the same ones used in Tables II and III. We find that the energy of substitution of F^- for Cl^- is -0.22 eV and the energy is 2.32 eV for the reverse process in the barium halides. For the strontium halides, the corresponding energies are -1.04 and 2.53 eV. These trends nicely correlate with ion size.

We now turn to the defect structure of the mixed halide alkaline-earth materials. We first consider sites where the interstitial ions are stable. A search of several locations in the crystal produced only one site where the defect was stable. This is near the center of a face containing Ba^{2+} and Br^- ions shown in Fig. 2. Approximate sketches show the final interstitial ion positions in this plane. Similar final positions are found in SrFCl and BaFCl. The energy of placing particular ions from infinity at this position is shown in Table VI. In addition, the vacancy energies resulting from removing a lattice ion to infinity are reported. These values may be combined to give Frenkel or Schottky defect energies. The Frenkel energy is just the sum of vacancy and interstitial formation energy for the appropriate ion. The

TABLE V. Energies of substitution (eV). Negative values refer to exothermic substitution reactions. $X^- = Br^-$ in BaFBr or Cl^- in BaFCl or SrFCl.

	BaFBr (Potential I)	BaFCl	SrFCl
F^- on X^- site	-1.12	-0.3	-2.2
X^- on F^- site	3.92	2.88	3.83

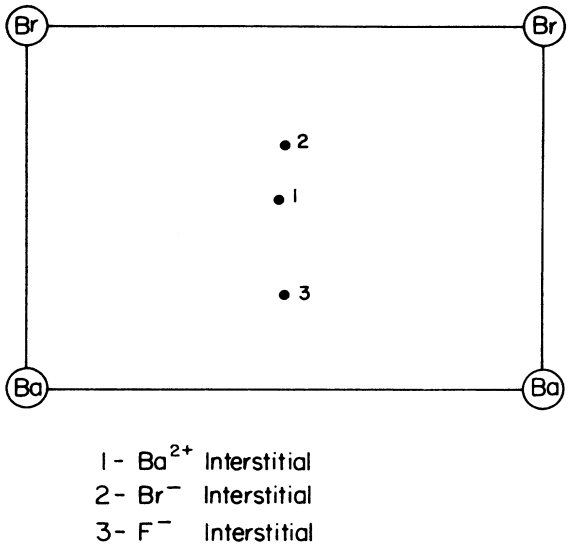

FIG. 2. A sketch of the stable position found for interstitial Ba^{2+}, F^-, and Br^- ions in BaFBr is shown for the plane containing Ba^{2+} and Br^- ions running parallel to the C axis.

Schottky energy results from subtracting the lattice energy from the sum of vacancy formation energies of each ion. It appears from these calculations that Frenkel defects on the halogen ion lattice are most easily formed in the intrinsic BaFCl, but that Schottky defects involving two chloride ion vacancies are more easily formed in SrFCl and BaFBr. Formation of the fluoride ion vacancies is energetically more difficult than for either the chloride or bromide ion vacancy throughout all of these materials. Thus vacancies are more easily formed on the chloride or bromide ion sites than on the fluoride ion sites. Various other defects involving F^- occupation of the larger halide ion site (antisites) might be considered and their energies of formation can be evaluated from the data in Table III. Generally either a Frenkel- or Schottky-type of defect, along with the appropriate antisite, has a larger defect energy than the normal Schottky or Frenkel defect energy. In the case of SrFCl, where two F^- ions occupy Cl^- sites and the defect consists of two F^- vacancies and one Sr^{2+} vacancy, the energy of formation is 4.1 eV which is smaller than the normal Schottky defect energy. The presence of such defects is certainly a possibility in these materials.

C. Hole centers in fluorohalides

The energetics of hole trapped species including V_k and H centers was investigated within a framework described recently[28] for a wide range of crystals. The hole is equally shared between two halogen species that act as a molecular anion. The interaction potential between the ions in this molecular species is determined from an electronic calculation. The molecular defect interacts with the rest of the crystal using short-range potentials identical to the interaction potentials between appropriate host ions. The Coulomb interactions are, of course, adjusted for the hole shared by the molecular anion. A detailed discussion of these approximations has been presented.[28]

We begin with the V_k center which consists of a hole equally shared between two adjacent halogen ions that have moved towards one another. This motion can be understood because now there is one less antibonding electron between the halide ion pair compared to the perfect crystal. Earlier[20] we have reported properties of the V_k center and noted that the formation energy $(E_D^0 + E_A)$ shown in Table VII (see Fig. 6 for definition of terms) represents the energy needed to remove an electron to infinity from the crystal with the associated relaxation of defect and host ions. We have consistently found the V_k center to have the lowest energy of formation for ions whose sites are in the two adjacent planes (termed out of plane) of like ions in the matlochkite structure. This is the Cl_2^- center in the SrFCl and BaFCl and Br_2^- in BaFBr. The most stable center contains one ion from each of the two adjacent planes giving an axis of the defect which makes approximately a 50°

TABLE VI. Computed defect energies (eV).

	BaFBr			
	I[a]	II[a]	BaFCl	SrFCl
Cation interstitial	−10.04	−6.69	−8.37	−7.20
F^- interstitial	−2.05	0.55	−2.48	−2.13
X^- interstitial	1.63	0.36	−1.59	0.51
Cation vacancy	19.67	18.84	19.55	19.74
F^- vacancy	6.40	6.31	6.29	6.33
X^- vacancy	4.07	3.42	4.36	3.32
Cation Frenkel	9.63	12.15	11.18	12.54
F^- Frenkel	4.35	4.33	3.81	4.20
X^- Frenkel	5.70	3.78	2.77	3.83
Schottky[b] (M, F^-, X^-)	6.34	6.02	6.40	5.49
Schottky[c] (M, $2X$)	4.01	3.08	4.47	2.48

[a]Appropriate potentials are shown in Table II.
[b]The Schottky defects consist of metal ion vacancies and two halogen ion vacancies of F^-, Cl^-, or Br^- type.
[c]This Schottky defect consists of one metal ion vacancy and two Br^- or Cl^- ion vacancies. Lattice energy is referenced to the mixed crystal.

TABLE VII. V_k defect energies (eV).

	E_D^{0}[c]	$E_D^0+E_A$[c]	V_k R_0 (Å)[d]	Crystal R (Å)[e]
		BaFBr		
F_2^-	7.08	11.21	2.02	3.19
FBr^-	5.15	8.53	2.58	3.45
Br_2^- in plane[a]	4.76	8.14	3.13	4.51
Br_2^- out of plane[b]	3.76	7.14	2.92	3.89
		BaFCl		
F_2^-	6.98	11.11	2.01	3.11
FCl^-	6.16	9.79	3.03	3.35
Cl_2^- in plane[a]	5.27	8.90	3.01	4.38
Cl_2^- out of plane[b]	4.43	8.06	2.83	3.77
		SrFCl		
F_2^-	7.24	11.37	2.01	2.92
FCl^-	7.63	11.26	2.52	3.25
Cl_2^- in plane[a]	5.17	8.80	2.98	4.09
Cl_2^- out of plane[b]	4.53	8.16	2.73	3.53

[a]In plane—both ions in same plane normal to C axis.
[b]Out of plane—both ions in different planes normal to C axis.
[c]See Fig. 6 for term definition.
[d]Distance of ions in V_k center.
[e]Distance of ions in crystal.

angle with the C axis. Experimentally, only this species has been observed by spin resonance[5] in single-crystal BaFCl. The Madelung potential at various crystal sites provides an explanation of the stability of this hole species as we have discussed.[20] The mixed halogen V_k centers originate from ions from different planes which are sketched in Fig. 1.

It is also apparent from Table VII that a significant relaxation of ions in the V_k center takes place. There is a reduction in distance of over 1 Å in many cases. This leads to significant movement of the surrounding host lattice ions. This is a complicated motion in a low-symmetry material such as we are considering here, but the most significant movements are shown in Fig. 3 for the stable Br_2^- V_k center. Note that Ba^{2+} ions move away from the V_k center as do the nearest Br^- ions and the nearest F^- ions to a smaller extent.

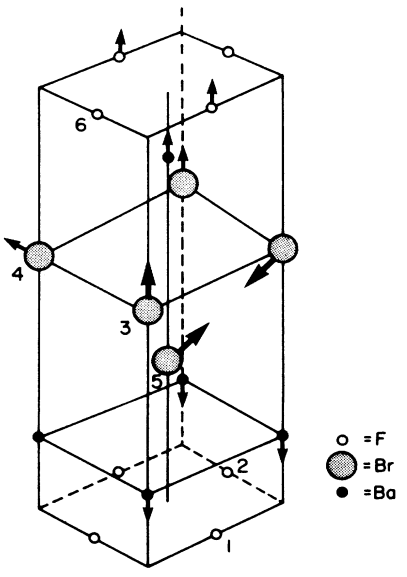

FIG. 3. A sketch of the host ion positions occurring around the most stable Br_2^- V_k center in BaFBr.

D. *H* centers in fluorohalides

The *H* center in alkaline-earth fluorohalides consists of a hole shared between an interstitial and a lattice halogen ion. The energetics of formation of this species is determined in Table VIII for the three materials considered in this report. A thermodynamic cycle is necessary to evaluate these formation energies. Figure 4 shows a cycle whereby an *H* center and the corresponding trapped electron species, the *F* center, is formed. This mechanism is similar to the exciton collapse process which has been discussed[29] in similar materials. The energy of placing a halogen atom in the lattice so as to form an *H* center (E_H) is smaller for F_2^- than Br_2^- *H*

TABLE VIII. *H*-center formation energies.

H center	E_H (eV)[a]	*F* (eV)[b]	ΔE (*F*-*H* pair) (eV)
		BaFBr	
F_2^-	2.78	−7.81	5.50
Br_2^-	3.93	−5.20	6.66
		BaFCl	
F_2^-	NC[c]	−6.39	
Cl_2^-	2.17	−5.97	4.19
		SrFCl	
F_2^-	3.59	−6.53	7.52
Cl_2^-	3.72	−6.23	4.44

[a]Energy of *H*-center formation.
[b]Ground-state energy of *F* center.
[c]Calculation not converged.

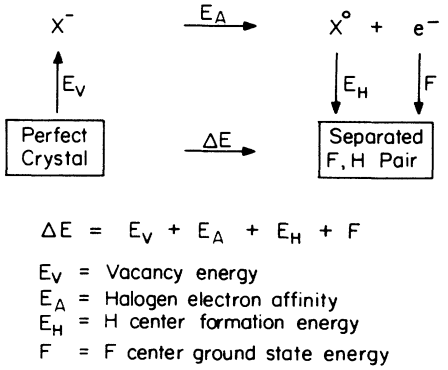

FIG. 4. A thermodynamic cycle showing the energy changes involved in *F-H* pair formation starting from the perfect crystal.

centers in BaFBr, but about equal in energy for F_2^- and Cl_2^- *H* centers in SrFCl. Corresponding values could not be determined in BaFCl because of nonconvergence of the F_2^- *H* center. The vacancy formation energy (E_V) and experimental atom electron affinity (E_A) are added to the *F* center energy to give the total energy of *F-H* pair formation. We employ energies of the *F* center ground state calculated for BaFCl and SrFCl by Lefrant and Harker[7] and using point-ion calculations for BaFBr.[30] Considerable amounts of energy are required to form the *F-H* center pairs shown in Table VIII, but these are less than the band-gap energy of BaFBr (8.3 eV) (Ref. 12) so that an exciton bound near the conduction band edge could decay to these pairs.

The configurations of *H* centers in BaFBr have been investigated after all ions are allowed to relax as shown in Fig. 5. In the case of the F_2^- *H* center, a (110) orientation is the low-energy geometry. Movement of F^- host ions in the plane away from the defect by $\sim 5\%$ of a lattice constant is found, while neighbor Ba^{2+} ions also move about 3% of a lattice constant away from the defect. In the case of the Br_2^- *H* center where the local symmetry is much lower than for F_2^- *H* centers, an off-center species is the low-energy form of *H* center. The *H* center is displaced along the C axis towards neighbor host Br^- ions and away from Ba^{2+} host ions. One particularly interesting *H* center structure is symmetrically located on the normal Br^- lattice site having a (111) type of orientation. This structure is 0.4 eV less stable than the structure shown in Fig. 5.

The orientation of the *H* centers can play an important role in decay of the self-trapped exciton since the exciton can initially be considered as an electron orbiting the *H* center.[31] In the case of the F_2^- center in Fig. 5, the axis is orientated away from the nearest neighbors making unhindered motion quite possible. The Br_2^- center in Fig. 5 has its axis almost along the nearest-neighbor direction which should tend to decrease its mobility. Thus unless a reorientation with low energy could occur, this *H* center would be less mobile than the F^{2-} *H* center. These considerations are important in determining recombination of electron and hole from the exciton center.

IV. DISCUSSION

We have applied the atomistic simulation techniques to the alkaline-earth mixed halides for the first time. It appears that suitable two-body potentials can be formed that do an adequate job of reproducing bulk crystal properties. The starting point for potential development involves use of well-known potentials in similar materials combined with electron-gas computed potentials. Then fitting procedures are used to minimize the lattice strain at the equilibrium crystal structure. The potentials we have developed in this manner provide useful simulations of the crystal under consideration. It is possible, however, that improvements could be made in potentials should experimental low-temperature elastic and dielectric constant data become available for these crystals.

Hole trapped defect species such as the V_k or *H* center are difficult to compare in relative stability because of the unknown role of the electron carrier. In Table VIII we consider formation of V_k centers from the perfect crystal with the corresponding electron at vacuum. In the case of *H* centers, as in Table VIII, the *H* center is formed from the perfect crystal with the electron trapped as an *F* center. This electron is trapped as an *F* center, because in the process of *H* center formation an anion vacancy is created, unlike the situation for

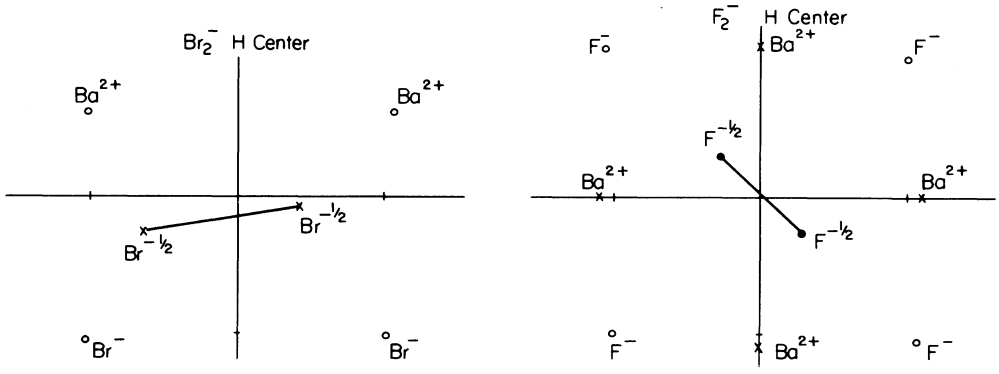

FIG. 5. Configurations of F_2^- and Br_2^- *H* centers in BaFBr showing relaxed positions of some of the neighboring host ions. Note that projected ion positions are shown for Br_2^- on the *a* and *c* axes and for F_2^- on the *a* and *b* axes.

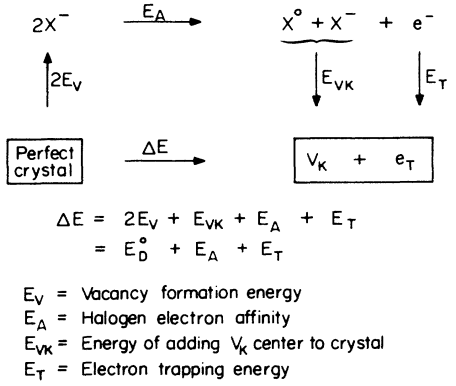

FIG. 6. A thermodynamic cycle showing the energy changes involved in V_k and trapped electron formation starting from the perfect crystal.

V_k center formation. If a concentration of electron trapping species exist in the crystal, then the electron formed concomitant with the V_k center will be trapped as shown in Fig. 6. This trapping species may be an impurity or perhaps an ionic defect. The trapping level relative to vacuum (E_T) would be needed in order to compare the relative stability of forming V_k and H centers.

We have noted that the computed energies of formation of Schottky defects and Frenkel defects on the Cl^- or Br^- lattice are close in value for the three materials considered. This makes it difficult to distinguish the predominant defect in the intrinsic material, since at any given temperature the fraction of ions in the form of defects, say halide ion vacancies, is

$$X_0=\left[\frac{A_s}{4}\right]^{1/3} e^{-E_s/3RT}, \qquad X_0=(A_F)^{1/2} e^{-E_F/2RT}, \tag{2}$$

as formed by Schottky and Frenkel defects, respectively. Clearly, knowledge of the pre-exponential factors A_s and A_F would be necessary to assess which mechanism provides the dominant defects. The pre-exponential factors are given by the entropy of defect formation

$$A = e^{\Delta S/R} \tag{3}$$

TABLE IX. Values of entropy of defect formation ($\Delta S/k$).

Defect	BaFBr Potential II
F^- Frenkel	−2.89
Br^- Frenkel	2.35
Schottky	−11.68
Schottky-$2Br^-$	−8.80

Temperature (K)	Fraction of defects Br^- Frenkel	$2Br^-$ Schottky
273	2.2×10^{-28}	4.2×10^{-21}
500	1.3×10^{-15}	1.6×10^{-12}
800	7.9×10^{-10}	1.2×10^{-7}

for both Frenkel or Schottky defects. We have computed the entropy of formation using a harmonic approximation involving the normal-mode frequencies of the perfect ω_i and defect ω_i' crystal. The entropy of formation in this approximation[32] is

$$S_v=-k\ln\left[\frac{\prod_i \omega_i'}{\prod_i \omega_i}\right], \tag{4}$$

and has been programmed.[33] The entropies of defect formation are enumerated in Table IX for the material BaFBr. We use these values in Eq. (2) to estimate the fraction of defects within a given lattice. We observe from Table IX that the Schottky-type defect involving two Br^- vacancies is predominant at the temperatures considered and possesses a rather large concentration with increasing temperature. Clearly the energy of defect formation is dominant in determining the defect structure.

ACKNOWLEDGMENTS

I am grateful to Raymond Eachus for many helpful conversations throughout the course of this work. I wish to thank A. M. Stoneham and C. R. A. Catlow for reading this manuscript and many helpful comments.

APPENDIX

The effect of region I size has been explored in our calculations. This region contains the ions relaxing ex-

TABLE X. Effect of region I size BaFBr—potential I.

Region I size	Ba^{2+} vacancy E_v [a]	E_v' [b]	Br_2^- V_k center E_{vk} [a]	E_{vk}' [b]
81	19.673	19.603	3.828	4.025
105	19.711	19.786	3.797	3.785
152	19.665	19.744	3.783	3.913
205	19.671	19.670	3.771	4.052

[a]Defect energy in fully relaxed crystal.
[b]Defect energy in strained crystal.

plicitly by the two-body potential. Table X shows the effect on the energy of formation of the Ba^{2+} vacancy and the Br_2^- out-of-plane V_k center in BaFBr. The formation energy becomes stable within 0.01 to 0.02 eV above 100 ions, which would certainly seem adequate for our calculation. This calculation is performed with a strain-free potential obtained by allowing the core and shell species to displace off center in the perfect crystal. We noted that some of our earlier calculations contained a perfect crystal with no core-shell displacement so that a residual energy was present. Table X compares the V_k defect energy computed in the latter mode and corrected for the residual energy with the result compared by allowing core-shell displacement in the perfect crystal. There is good agreement at particular sizes, but this is not always true. Thus we concluded that the relaxed structure, having separated core and shell species for each ion, is a better starting point for these calculations.

[1]B. W. Liebich and P. Nicollin, Acta. Crystallogr. Sec. B **33**, 2790 (1977).
[2]H. P. Beck, J. Solid State Chem. **17**, 275 (1976).
[3]E. Nicklaus and F. Fisher, Phys. Status Solidi B **52**, 453 (1972).
[4]J. R. Niklas, G. Herder, M. Yuste, and J. M. Spaeth, Solid State Commun. **26**, 169 (1978).
[5]M. Yuste, L. Taurel, and M. Rahmani, Solid State Commun. **17**, 1435 (1975).
[6]R. U. Bauer, J. R. Niklas, and J. M. Spaeth, Phys. Status Solidi B **118**, 557 (1983).
[7]S. Lefrant and A. H. Harker, Solid State Commun. **26**, 169 (1978).
[8]K. R. Balasubramaian, T. M. Hardison, and N. Krishnamurthy, Solid State Commun. **32**, 1095 (1979).
[9]M. Sieskind, M. Ayadi, and G. Zachmann, Phys. Status Solidi B **136**, 489 (1986).
[10]K. R. Balasubramaian, T. M. Haridasan, and N. Krishnamurthy, Chem. Phys. Lett. **67**, 530 (1979).
[11]J. L. Sommerdijk, J. M. P. Verstegen, and A. Bril, J. Lumin. **8**, 502 (1974).
[12]K. Takahashi, K. Kohda, J. Miyahara, Y. Kanemitsu, K. Amitani, and S. Shionoya, J. Lumin. **31**, 266 (1984).
[13]K. Takahashi and J. Miyahara, J. Electrochem. Soc. **132**, 1492 (1984).
[14]Y. Kondo, M. Hirai, and M. Yeta, J. Phys. Soc. Jpn. **33**, 151 (1972).
[15]J. N. Bradford, R. T. Williams, and W. L. Faust, Phys. Rev. Lett. **35**, 300 (1975).
[16]C. H. Leung and K. S. Song, Phys. Rev. B **18**, 922 (1978).
[17]C. H. Leung and K. S. Song, Can. J. Phys. **58**, 412 (1980).
[18]C. R. A. Catlow, M. Dixon, and W. C. Mackrodt, *Computer Simulation of Solids* (Springer-Verlag, Berlin, 1982).
[19]M. J. Norgett, Atomic Energy Research Establishment Report No. AERE-R7650 (1974) (unpublished).
[20]R. C. Baetzold and R. S. Eachus, Proceedings of the 5th Europhysical Topical Conference on Lattice Defects in Ionic Crystals, 1986 (unpublished).
[21]B. G. Dick and A. W. Overhauser, Phys. Rev. **112**, 90 (1958).
[22]A. M. Stoneham and J. H. Harding, Ann. Rev. Phys. Chem. **53**, 80 (1986).
[23]C. R. A. Catlow, M. J. Norgett, and T. A. Ross, J. Phys. C **10**, 1627 (1977); C. R. A. Catlow, *ibid.* **12**, 969 (1979).
[24]R. G. Gordon and Y. S. Kim, J. Chem. Phys. **56**, 3122 (1972); **60**, 1842 (1974).
[25]A. M. Stoneham, Atomic Energy Research Establishment Report No. R9598 (1981) (unpublished).
[26]M. Sieskind and M. Ayadi, J. Solid State Chem. **49**, 188 (1983).
[27]P. Herzig, J. Solid State Chem. **57**, 379 (1985).
[28]P. E. Cade, A. M. Stoneham, and P. W. Tasker, Phys. Rev. B **30**, 4621 (1984).
[29]L. W. Hobbs, *Surface and Defect Properties of Solids Specialist Periodical Reports,* edited by J. M. Thomas and M. W. Roberts (The Royal Society of Chemistry, London, 1975), Vol. 4, p. 152; N. Itoh, A. M. Stoneham, and A. H. Harker, J. Phys. C **10**, 4197 (1977).
[30]R. C. Baetzold (unpublished); see Ref. 17 for method of calculation.
[31]K. S. Song, A. M. Stoneham, and A. H. Harker, J. Phys. C **8**, 1125 (1975).
[32]J. H. Harding, Phys. Rev. B **32**, 6861 (1985).
[33]J. H. Harding, SHEOL code.